Applied Physics Letters

Measurement of interface potential change and space charge region across metal/organic/metal structures using Kelvin probe force microscopy

Cite as: Appl. Phys. Lett. **85**, 4148 (2004); https://doi.org/10.1063/1.1811805
Submitted: 06 May 2004 . Accepted: 30 August 2004 . Published Online: 03 November 2004

O. Tal, W. Gao, C. K. Chan, A. Kahn, and Y. Rosenwaks

View Online

Export Citation

ARTICLES YOU MAY BE INTERESTED IN

Kelvin probe force microscopy
Applied Physics Letters **58**, 2921 (1991); https://doi.org/10.1063/1.105227

Resolution and contrast in Kelvin probe force microscopy
Journal of Applied Physics **84**, 1168 (1998); https://doi.org/10.1063/1.368181

Nonuniform doping distribution along silicon nanowires measured by Kelvin probe force microscopy and scanning photocurrent microscopy
Applied Physics Letters **95**, 092105 (2009); https://doi.org/10.1063/1.3207887

Lock-in Amplifiers
Zurich Instruments
Watch the Video

AIP Publishing

© 2004 American Institute of Physics.

HTML ABSTRACT * LINKS

Measurement of interface potential change and space charge region across metal/organic/metal structures using Kelvin probe force microscopy

O. Tal
Department of Physical Electronics, Faculty of Engineering, Tel Aviv University, Tel Aviv 69978, Israel

W. Gao,[a] C. K. Chan, and A. Kahn
Department of Electrical Engineering, Princeton University, Princeton, New Jersey 08544

Y. Rosenwaks[b]
Department of Physical Electronics, Faculty of Engineering, Tel Aviv University, Tel Aviv 69978, Israel

(Received 6 May 2004; accepted 30 August 2004)

We report on high-resolution potential measurements across complete metal/organic molecular semiconductor/metal structures using Kelvin probe force microscopy in inert atmosphere. It is found that the potential distribution at the metal/organic interfaces is in agreement with an interfacial abrupt potential changes and the work function of the different metals. The potential distribution across the organic layer strongly depends on its purification. In pure Alq_3 the potential profile is flat, while in nonpurified layers there is substantial potential bending probably due to the presence of deep traps. The effect of the measuring tip is calculated and discussed. © *2004 American Institute of Physics*. [DOI: 10.1063/1.1811805]

The performance of organic electronic devices depend, to a large extent, on the potential profile across the device and its interfaces. There is considerable interest in understanding the physical origin and location of potential shifts across the device, as these can occur through interface dipoles, or band bending (either from band tail states[1] or trapped charges) or both; hence accurate potential distribution measurements are of considerable importance. To date, measurements of molecular energy levels and level offsets across metal-organic and organic-organic interfaces have been carried out by ultraviolet photoemission spectroscopy (UPS),[2–4] x-ray photoemission spectroscopy (XPS)[5] and Kelvin probe (KP)[6] measurements as a function of organic layer thickness. Yet, potential profiles, across interfaces and complete devices can only be inferred from Kelvin probe force microscopy (KPFM) measurements.

Many groups have used KPFM to study potential distributions across inorganic semiconductor[7,8] but there are very few studies performed on organic devices.[9,10] In the case of inorganic semiconductors, surface charges associated with gap states are present at most surfaces and limit the usefulness of KPFM on cross-section investigations. On the other hand, surface states are generally absent in van-der-Waals bonded molecular materials, making KPFM particularly suitable for the latter. We present here a study of the potential profile across $Au-Alq_3-M$ layered structures (Alq_3: tris (8-hydroxy-quinoline) aluminum; M: Au, Al, no metal) performed in a nitrogen environment with nanometer spatial resolution afforded by KPFM. We compared the fine features of the potential profile with the results obtained via UPS.

GaAs/Cr(5 nm)/Au(50 nm)/Alq_3(1–3 μm)/M structures (Fig. 1 Inset) were prepared by sublimation from solid sources in an ultrahigh vacuum (UHV) growth chamber in Princeton University and transported under nitrogen atmosphere to the KPFM glovebox at Tel Aviv University. The GaAs wafer serves as a cleavable mechanical substrate. A few nm of clean Au were evaporated in UHV on this initial Au layer (for a total thickness of 50 nm) to provide a bottom metal surface with high work function. The organic layer and the top metal layer were then deposited in the same UHV chamber.

Our KPFM[11] (Autoprobe CP—Veeco Inc.—with Kelvin probe homemade electronics[12]) was placed inside a homebuilt glovebox with nitrogen atmosphere (<2 ppm water). The samples were cleaved *in situ* shortly before the KPFM measurements in the dark.[13] The samples were scanned in noncontact mode near the cleaved edge, and the contact potential difference (CPD) measurements were typically performed on a relatively smooth cleavage area, with a small metal stretching, continuous layers, and a small roughness of the organic layer.

Figure 1 shows a topography image and a CPD profile of a typical layered structure. The GaAs substrate is on the left and the Alq_3 is placed between two gold layers on the right (see also the inset). The sandwich-like structure can be easily recognized due to the protrusion of the two metals (110 nm with respect to the organic surface). These protrusions are due to differences in the mechanical properties of the different layers and to low adhesion at the interfaces, which lead to an inherent effect of stretching the metal layers over the GaAs edge during the cleavage process.

The CPD profile in the proximity of the Au/Alq_3 junctions in Fig. 1, i.e., the ~600 meV step down on the left and ~600 meV step up on the right, can be attributed to the interface electric dipole at these junctions.[14] The constant CPD between the metal contacts indicates that the molecular energy levels are flat across the organic bulk. The two peaks observed on the inner Au layer are attributed to a lowering of the Au work function due to exposure of the GaAs/Cr/Au substrate to air[15,16] prior to UHV deposition of the rest of the structure (i.e., Au/Alq_3/Au). UPS measurements generally show a 0.9–1.25 eV interface dipole and drop in vacuum level energy upon evaporation of the first molecular layer of

[a]Now at: Central Research and Development, Wilmington, DE, 19880.
[b]Author to whom correspondence should be addressed; electronic mail: yossir@eng.tau.ac.il

 © 2004 American Institute of Physics

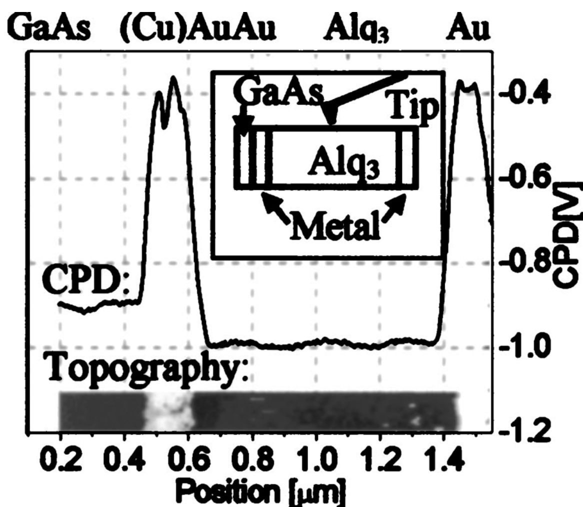

FIG. 1. CPD profile of left to right cross sections of a GaAs/(Cr)/Au/Au/(purified) Alq3/Au layered structure. Bottom inset presents topography image of the relevant area. Top inset shows schematics of the tip-cleaved sample geometry.

Alq_3 on clean Au, as illustrated in the energy levels scheme shown in Fig. 2(a).[3,14,17,18] The smaller potential drop (~600 meV) measured by the KPFM on this interface (Fig. 1) is probably due to the fact that the Au on the "cleaved" surface is exposed to residual water and oxygen impurities in the glovebox and thus has a lower work function than the Au measured with UPS in UHV. Such a contamination of Au by oxygen and water can decrease its work function by up to about 1 eV.[15,16] Figure 1 also shows that the potential shifts at the two Au/Alq_3 interfaces are ~65 nm wide, considerably more than observed via UPS. This is a measure of the KPFM resolution near a protruding metal layer, and is a consequence of the tip averaging effect, which will be analyzed in details below.

Figure 3 shows a CPD profile (solid curve) measured across a structure comprising an inner gold layer (left) and an outer aluminum layer (right), as shown in Fig. 2(b). In addition to the dipole-related potential drops at the two interfaces, there is a potential drop between the gold and the aluminum layers due to the difference in their work functions. This is illustrated in the UPS based energy level diagram in Fig. 2(b). Figure 3 also shows a comparison between CPD profiles measured on $GaAs/(Cr)Au/Alq_3/Al$ (solid curve) and $GaAs/(Cr)Au/Alq_3$ (dashed curve) structures. In the later case the outer aluminum layer was pilled off during the cleavage. The abrupt potential change at the outer (right) Alq_3/Al interface clearly affects the whole potential distribution across the organic layer in comparison to the case of no

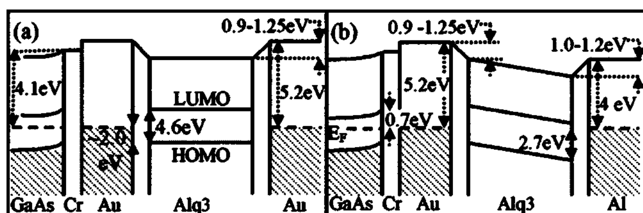

FIG. 2. Schematic energy levels structure (not in scale) based on UPS and inverse photoemission spectroscopy measurements (see Refs. 3, 14, 17, and 18) for (a) $GaAs/(Cr)/Au/Au/Alq_3/Au$ structure, and (b) $GaAs/(Cr)/Au/Au/Alq_3/Al$ structure. The data for GaAs (100)/Cr were taken from Ref. 9. For the Alq_3 flat energy levels were assumed.

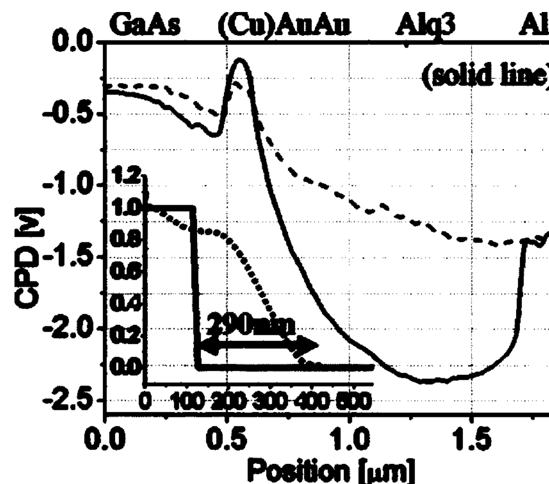

FIG. 3. Potential profile measured across $GaAs/(Cr)/Au/Alq_3/Al$ (solid line) and $GaAs/(Cr)/Au/Alq_3$ (dashed line) structures. The inset demonstrates the averaging effect of the tip by showing a calculated CPD (dashed) for a metal strip (solid) at a potential 1 V higher than the surface.

outer Al layer where no abrupt potential change is observed. The fact that the two CPD curves merge at the outer border on the Alq_3 layer may stem from aluminum residuals (left after cleavage) that "pin" the potential but do not support a macroscopic potential drop. The inset is a calculation of the tip electrostatic averaging effect explained in the next section.

The measured CPD equals the tip voltage that minimizes the electrostatic force between the tip and the sample. Due to the long-range electrostatic force, the measured CPD at a point on the surface below the tip apex is a weighted average of the surface potential in the vicinity of the tip. The effect here is even stronger since the two metallic layers, which have work function considerably different from that of the molecular layer, also protrude from the sample surface, affecting the tip-sample electrostatic interaction.

The effect of the tip electrostatic averaging was calculated as follows. The three-dimensional Laplace equation was solved (using a finite element commercial code) for the following system. A metallic tip (cone shaped with a hemispherical apex, tip height: 5 μm, tip opening angle: 11.3°, and apex radius of curvature of 20 nm) located 20 nm above a surface composed from a flat region representing the organic layer at a potential of 0 V, and a protruding square strip (160 nm high and 160 nm wide) representing one of the metal contacts at a potential of 1 V; this strip represents the ~1 V potential step at the Au/Alq_3 interface. For each tip location, the potential was calculated for three different tip voltages, and the CPD was extracted in the following way. The electrostatic force between the tip and the surface was calculated by integrating the Maxwell stress over the entire tip surface.[19] $F_z = -\frac{1}{2}\varepsilon \oint_{\text{tip surface}} E_z \hat{z} E_n d\hat{n}$, where $d\hat{n}$ is a tip surface element normal to the surface, $\hat{z}$ is a unit vector in the z direction (tip-axis direction), ε is the dielectric constant, and the integral is calculated over the entire tip surface. The electrostatic force was then expanded[20] as $F_z = a_1 + a_2 V + a_3 V^2$ to yield the voltage that minimizes the force (i.e., the CPD) through $V_{\min} = -a_2/2a_3$.

The results are shown in Fig. 3 inset. The calculated step-like CPD profile (dashed curve) is widened by the measuring tip to a step ~290 nm wide which is larger then experimentally observed (see Fig. 2). The calculated CPD

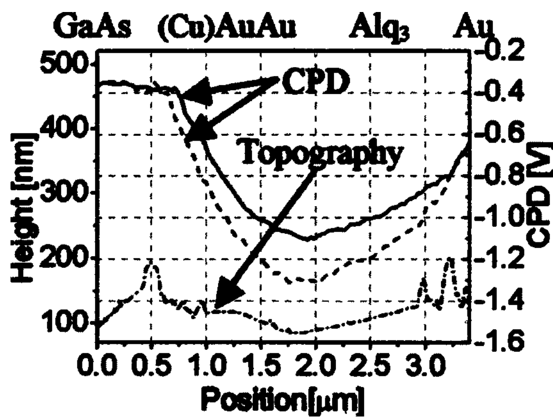

FIG. 4. CPD profile measured across GaAS/(Cr)/Au/(nonpurified) Alq_3/Au structure under zero bias. Solid and dashed curves were before and after applying a bias, respectively. Dotted curve: Topography profile.

shape at the metal strip corner is attributed to the electrostatic interaction when the tip apex is in proximity to the step corner. Comparing this calculation with the dashed curve (no top Al layer) in Fig. 3 at a distance 290 nm away from the junctions, we conclude that the curvature in the measured CPD may be solely due to a tip broadening of the abrupt potential drop at the Au/Alq_3 interface.

Figure 4 shows a CPD profile measured on a GaAs/(Cu)Au/Alq_3/Au structure. The upper (solid) potential profile is concave, in contrast to the profile in Fig. 1, which is nearly flat across the Alq_3 layer. This interesting difference is presumably due to the different impurity contents of the two Alq_3 layers; the Alq_3 material used in the device measured in Fig. 4 was not purified before deposition, while the Alq_3 used in the device measured in Fig. 1 was purified by multiple cycles of gradient sublimation. In the case of unpurified Alq_3, unintentional doping is likely to introduce traps with a broad energy distribution.[21] Such traps may give rise to a space charge region (SCR), causing the observed curved CPD profile. The presence of a SCR is also consistent with the simulation results, since the concave shape of the CPD profiles also appears at distances much larger then 290 nm from the two contacts; thus the tip averaging effect is not likely to be the origin for the curved potential profile. The effect of unintentional doping on SCR was also demonstrated by Kelvin probe measurements on C_{60} as a function of film thickness. Hayashi *et al.* showed an enhanced molecular level bending across a 600-nm-thick C_{60} layer deposited on copper from as-received material as compared to purified C_{60}.

Finally, applying a 1 V bias for 2 min between two consecutive CPD measurements, conducted at zero bias, lowers the CPD profile (dashed curve in Fig. 4). A similar structure that contained purified Alq_3 did not show any such changes in CPD. The applied bias induces positive charging of deep traps in the Alq_3 layer and thus lowers the local vacuum level, lowest unoccupied molecular orbital and highest occupied molecular orbital energies; as reflected in the lower CPD across the Alq_3 layer.

In summary, we have measured potential profiles on a complete metal/organic/metal layered structures using Kelvin probe force microscopy. The abrupt potential drops across the metal/organic interfaces, which are often ascribed to interfacial potential dipole, and the influence of the different metal work functions, were clearly observed. Using numerical analysis, we estimated the broadening effect introduced by the tip for KPFM measurement on samples that exhibits abrupt potential and topographical steps. We conclude that nonpurified Alq_3 layers between two metal contacts sustain molecular level bending, in contrast to purified Alq_3 (within our measurement resolution), which was explained by the presence of deep traps in nonpurified Alq_3.

This research was generously supported by US-Israel Binominal Science Foundation (BSF), Grant No. 2000-092.

[1]G. Paasch, H. Peisert, M. Knupfer, J. Fink, and S. Scheinert, J. Appl. Phys. **93**, 6084 (2003).
[2]A. Kahn, N. Koch, and G. Weiying, J. Polym. Sci., Part B: Polym. Phys. **41**, 2529 (2003).
[3]H. Ishii, K. Sugiyama, E. Ito, and K. Seki, Adv. Mater. (Weinheim, Ger.) **11**, 605 (1999).
[4]H. Ishii and K. Seki, IEEE Trans. Electron Devices **44**, 1295 (1997).
[5]W. D. Grobman and E. E. Koch, *Photoemission in Solids*, edited by L. Ley and M. Cardona (Springer, Berlin, 1979), Vol. 2, p. 261.
[6]K. Seki, H. Oji, N. Hayashi, Y. Ouchi, and H. Ishii, Proc. SPIE **3797**, 178 (1999).
[7]R. Shikler, T. Meoded, N. Fried, and Y. Rosenwaks, Phys. Rev. B **61**, 11041 (2000).
[8]R. Shikler, T. Meoded, N. Fried, and Y. Rosenwaks, J. Appl. Phys. **86**, 107 (1999).
[9]L. Burgi, T. J. Richards, R. H. Friend, and H. Sirringhaus, J. Appl. Phys. **94**, 6129 (2003).
[10]L. Burgi, H. Sirringhaus, and R. H. Friend, Appl. Phys. Lett. **80**, 16 (2002).
[11]M. Nonnenmacher, M. P. O'Boyle, and H. K. Wickramasinghe, Appl. Phys. Lett. **58**, 2921 (1991).
[12]R. Shikler, T. Meoded, N. Fried, and Y. Rosenwaks, Appl. Phys. Lett. **74**, 2972 (1999).
[13]Except for the AFM feedback laser, which operates at 1.85 eV, smaller then the optical gap of Alq_3 ($\sim$3.2 eV) but larger than the metal Alq_3 barriers. Sample illumination was minimized by tip shielding and reducing the laser intensity; no changes in CPD were observed using different laser intensities.
[14]C. Shen and A. Kahn, Org. Electron. **2**, 89 (2001).
[15]S. C. Fain, Jr., L. V. Corbin II, and J. M. McDavid, Rev. Sci. Instrum. **47**, 345 (1976).
[16]J. M. Heras and E. V. Albano, Z. Phys. Chem., Neue Folge **129**, 11 (1982).
[17]I. G. Hill, A. Kahn, Z. G. Soos, and R. A. Pascal, Jr., Chem. Phys. Lett. **327**, 3 (2000).
[18]A. Rajagopal, C. I. Wu, and A. Kahn, J. Appl. Phys. **83**, 2649 (1998).
[19]S. Belaidi, F. Lebon, P. Girard, G. Leveque, and S. Pagano, Appl. Phys. A: Mater. Sci. Process. **66**, S239 (1998).
[20]S. Hudlet, M. Saint Jean, B. Roulet, J. Berger, and C. Guthmann, J. Appl. Phys. **59**, 3308 (1995).
[21]S. Karg, J. Steiger, and H. von Seggern, Synth. Met. **111**, 277 (2000).